Arch. Metall. Mater., Vol. 61 (2016), No 2, p. 753–760

DOI: 10.1515/amm-2016-0128

A. ZIELIŃSKI*, M. SROKA**#, M. MICZKA*, A. ŚLIWA**

FORECASTING THE PARTICLE DIAMETER SIZE DISTRIBUTION IN P92 (X10CrWMoVNb9-2) STEEL AFTER LONG-TERM AGEING AT 600 AND 650 °C

The investigations on microstructure of P92 steel in the as-received condition and after 10^5 h ageing at 600 and 650 °C were carried out. For the recorded images of microstructure, the quantitative analysis of precipitates was performed. On that basis, a statistical analysis of collected data was made with the aim of estimating parameters of selected theoretical statistical distribution. Then, the forecast for average precipitate diameter and standard deviation of such a distribution for the time of $1{,}5*10^5$h at 600 and 650 °C was calculated. The obtained results of investigations confirm the possibility of using, in evaluation of degradation degree for materials in use, the forecasting methods derived from mathematical statistics, in particular the theory of stochastic processes and methods of forecasting by analogy.

Keywords: P92 steel, microstructure, precipitates, statistics, forecasting

1. Introduction

The T/P92 (X10CrWMoVNb9-2) is a high-temperature martensitic steel from the group of 9%Cr content steels used for hot-rolled seamless tubes to be operated at up to 620 °C. It was produced by modification and optimisation of the chemical composition of P91 steel, mainly by adding 1.8% tungsten as well as niobium, boron and nitrogen microadditions, and by reduction in molybdenum content down to 0.6% [1]. This steel has filled the gap between the materials for service at elevated temperature under subcritical load conditions and the alloys that may transfer supercritical and ultra-supercritical load conditions [2-4]. It is characterised by a number of significant features, including, but not limited to, good strength properties, corrosion resistance, weldability and heat resistance at elevated temperature, and much higher, by approx. 20%, creep strength compared to the X10CrMoVNb9-1 (T/P91) steel.

Long-term impact of elevated temperature during the operation of pressure equipment and systems brings about changes in the microstructure of the material resulting in reduction of mechanical properties [5-9]. These changes determine the life time of components, which are now designed for $2*10^5$ h of operation. However, it does not indicate that a failure-free operation is ensured for such a long time [6].

The knowledge of the impact of temperature on a change in the mechanical properties and microstructure is used for correct evaluation of material condition, not only during its service within the design time, but also beyond it [10-14].

The dynamics of changes in microstructure is determined by the working temperature level, and such changes are additionally accelerated by stress due to pressure in the system.

In this paper, the statistical methods were used to calculate the forecast precipitate diameter distribution for P92 steel in the as-received condition and for ageing duration of 10^3, 10^4, $7*10^4$ and 10^5 h at 600 and 650 °C.

The use of such methods may be considered as a verification of and supplement to the most often used models derived from the theory of thermodynamics, which describe the development of the carbide precipitation process in steel. The basic models include:

a) average precipitate radius approximation,
b) Euler approximation for multiple classes of precipitates,
c) Lagrange approximation for multiple classes of precipitates.

They allow the quantitative description of a development of precipitates over time including their parameters [15].

The proposed data analysis and forecast procedure consists in evaluating, based on collected data, the theoretical log-normal distribution parameters and using these evaluations for calculation of forecast about both measures of location and distribution. This allows the entire statistical distribution to be calculated for the assumed point in time, and thus to obtain more complete information necessary to take decisions than for the classic mean value forecast.

The results of investigations with the same research methodology used were carried out for the T24 steel, and investigations on the T23, P92 and VM12 steels are in progress [16-19].

1.1. Material for investigations

The material for investigations was test pieces of P92 (X10CrWMoVNb9-2) steel in the as-received condition and

* INSTITUTE FOR FERROUS METALLURGY, GLIWICE, POLAND

** SILESIAN UNIVERSITY OF TECHNOLOGY, INSTITUTE OF ENGINEERING MATERIALS AND BIOMATERIALS, FACULTY OF MECHANICAL ENGINEERING, 18A KONARSKIEGO STR., GLIWICE 44-100, POLAND

Corresponding author: marek.sroka@polsl.pl

after long-term ageing for 10^3, 10^4, $7*10^4$ and 10^5 hours. The composition of the examined steel meets the requirements of [21].

2. Methodology of investigations

The microstructural investigations were carried out with a scanning electron microscope (SEM) Inspect F on conventionally prepared nital-etched metallographic microsections.

The quantitative analysis of precipitates was carried out using the image analysis system NIKON EPIPHOT200 & LUCIA G v.5.03. The image analysis system was calibrated using the scale marker placed in structure images. Calibration coefficient: 1 pixel= 0.040 μm. A measuring frame of 1020 x 940 pixels was applied to every analysed image.

A statistical analysis of collected data aimed at estimation of parameters of selected theoretical statistical distribution followed by the calculation of a forecast of the expected value and standard deviation of such a distribution was made for the time of 10^5 h. Finally, a forecast was made for the entire distribution based on the assumption that it took the form of a log-normal distribution.

2.1. Density forecasting

A density forecast of the realization of a random variable (diameter of precipitates) at some future time is an estimate of the probability distribution of possible future values of that variable. Thus, it provides a complete description of the uncertainty associated with a prediction and stands in contrast to a point forecast which by itself contains no description of the associated uncertainty. The intermediate between these two extremes is a prediction interval which specifies the probability that the actual outcome will fall within a defined interval. To report a prediction interval represents the first response by point forecasters to the criticism of their silence on the subject of uncertainty. This feature is very important in the area of failure risk assessment, in particular the risk of material damage.

3. Results of investigations

3.1. Microstructure

The purpose of the microstructure investigations using a scanning electron microscope was to reveal the microstructure of the examined steel both in the as-received condition and after ageing at 600 and 650 °C for 10^3, 10^4, $7*10^4$ and 10^5 hours. For the above assumed material conditions, from 10 to 15 images of microstructure were recorded at a magnification of 2000 x. The examples of these images are shown in Figs. 1 through 3.

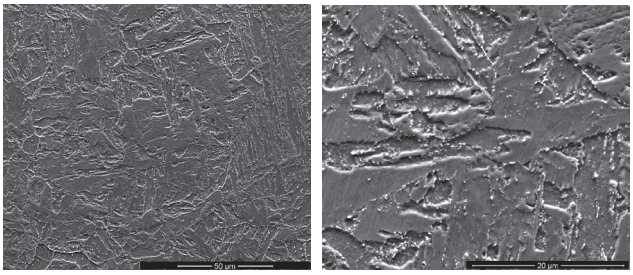

Fig. 1. Structure of P92 steel in the as-received condition

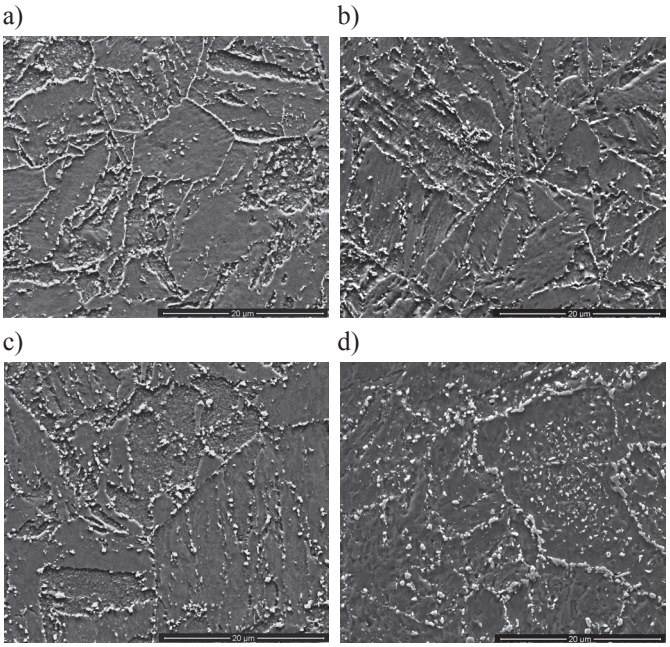

Fig. 2. Structure of P92 steel after ageing at 600 °C for, a) 10^3 h, b) 10^4 h, c)$7*10^4$ h, d) 10^5 h

In its as-received condition, the P92 steel is characterised by the tempered lath martensite microstructure, typical of this group of steels (Fig. 1). The X-ray phase composition analysis of precipitates confirms the existence of MX and $M_{23}C_6$ precipitates in the examined steel in the as-received condition [20].

Characteristic images of the structure after ageing at 600 and 650 ºC are presented in Figs. 2-3. No significant changes in the image of microstructure of the examined steel with reference to its as-received condition were observed after ageing at 600 and 650 ºC for 10^3 h (Figs. 2a,3a).

TABLE 1

Chemical composition of the P92 steel, wt%

Chemical composition, % mass.												
-	C	Mn	Si	P	S	Cr	Mo	V	W	Nb	B	N
As tested	0.10	0.45	0.17	0.01	0.01	9.26	0.47	0.20	1.95	0.059	0.009	0.04
PN-EN 10216-2:2009	0.07-0.13	0.30-0.60	max 0.50	max 0.02	max 0.01	8.5-9.5	0.30-0.60	0.15-0.25	1.5-2.0	0.04-0.09	max 0.006	0.03-0.07

Visible changes in the image of microstructure compared to the as-received condition were observed on test pieces aged for 10^4 h (Figs. 2b,3b). The increase in the size of precipitates was found after that time of annealing. As it should have been expected, their size was bigger after long-term annealing at 650 ºC (Fig. 3b). In the microstructure of P92 steel after 10^4 h annealing, the effects of progressing tempered martensite processes can be observed. They result in bigger and more densely arranged $M_{23}C_6$ carbide precipitates at the former austenite grain boundaries and martensite laths. After annealing at 650 ºC, the local disappearance of lath martensite structure is observed.

The extension of the duration of ageing at 600 °C up to $7*10^4$ h resulted in increase in the size of precipitates (Fig. 2c), while the microstructure image of the tested steel aged for $7*10^4$ h/650 °C shows, in addition to the coagulation of precipitates, a further atrophy of the martensite lath structure (Fig. 3c). This microstructure was characterised by partially degraded martensite with large-size carbide precipitates at the former austenite grain boundaries, martensite laths and inside grains.

The microstructure of P92 steel after annealing at 600 °C for 10^5 h was characterised by a partial disappearance of the martensite lath structure and advanced precipitation process at the former austenite grain boundaries and martensite laths. It manifests itself in the increase and coagulation of precipitates that form chains at the former austenite grain boundaries (Fig. 2d). The highest degree of degradation for P92 steel was observed after aging for 10^5 h/650 °C, which is shown in Fig. 3d. This microstructure is distinguished by precipitates with the biggest diameter and greatest disappearance of the lath martensite structure.

The recorded images of microstructure were used to carry out the quantitative analysis of the diameter of precipitates occurring mainly at the former austenite grain boundaries and martensite laths. According to the literature data confirmed by results of own research, there are mainly $M_{23}C_6$ carbides in these areas within the examined steel after long-term ageing [16].

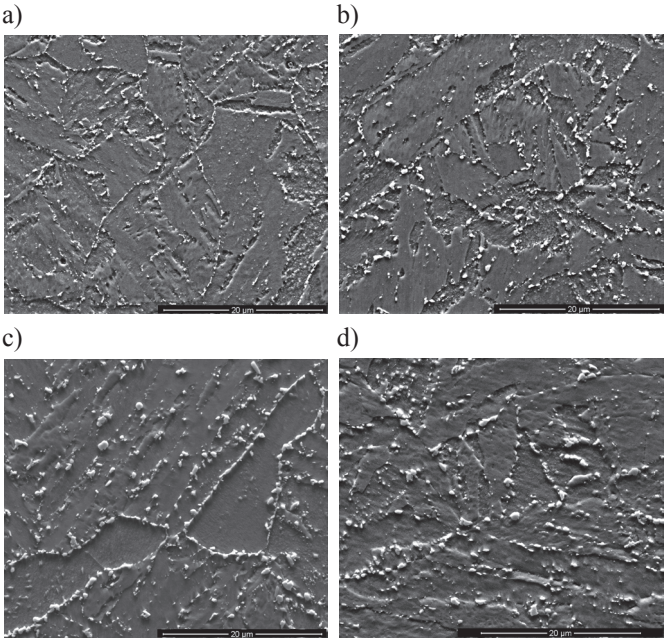

Fig. 3. Structure of P92 steel after ageing at 650 °C for, a) 10^3 h, b) 10^4 h, c)$7*10^4$ h, d)10^5 h

The basic statistical measures that describe the structure of the data set are presented in Table 2. The results in the form of distributions of equivalent diameters of the existing precipitates for the analysed conditions of the examined P92.

The collected results of investigations were the basis for carrying out the statistical analysis of the set's structure to adopt the assumption on the form of the probability density function.

3.2. Non-parametric estimation, kernel density estimators

With the knowledge of the basic measures of location, variability (dispersion), asymmetry and concentration, you can move on to the estimation of theoretical distributions of the analysed variables. Parametric and non-parametric estimation

TABLE 2

Basic statistical measures describing the structure of the data set

Material condition	Average	St. dev.	Var. Coeff.	Skewness	Kurtosis	Quart. 1 25%	Median 50%	Quart. 2 75%
As-received	0.178	0.061	34.3%	0.765	3.010	0.127	0.162	0.216
600 °C/1	0.287	0.146	50.9%	1.355	4.761	0.180	0.247	0.355
600 °C /10	0.320	0.159	49.7%	1.426	5.506	0.202	0.276	0.404
600 °C /70	0.337	0.166	49.3%	1.179	4.218	0.207	0.296	0.416
600 °C /100	0.345	0.187	54.1%	1.219	4.186	0.197	0.281	0.453
650 °C /1	0.316	0.155	49.1%	1.448	5.339	0.199	0.274	0.380
650 °C /10	0.342	0.185	54.1%	1.519	5.697	0.212	0.281	0.432
650 °C /70	0.352	0.181	51.3%	1.433	6.141	0.212	0.306	0.449
650 °C /100	0.412	0.206	50.0%	1.879	8.118	0.281	0.352	0.486

methods serve this purpose. The parametric estimation can be applied when the class of distributions that the distribution of the examined variable belongs to is known. If the analytical form is unknown, the non-parametric methods are used. Below, an attempt of using both the approaches is made. First, the non-parametric estimation was used to determine the analytical class of the probability density function [21].

If $f(x)$ is the distribution density of variable X, whereas $x_1, x_2, \ldots, x_n$ is a simple sample taken from the general population, the kernel density estimator is a function in the form *(1)* [22]:

$$f_n(x, a_n) = \frac{a_n}{n} \sum_{i=1}^{n} K[a_n(x - x_i)] \quad (1)$$

where: a_n- definitely divergent sequence of positive numbers.

The function $K(\cdot)$ was assumed to be in the form of the Epanechnikov kernel *(2)* [21]:

$$K(x) = \begin{cases} \frac{3}{4}(1 - x^2) \text{ for } x \in [-1,1] \\ 0 \text{ for } x \in (-\infty, -1) \cup (1, \infty) \end{cases} \quad (2)$$

The histogram and density function fitting are presented in Figs. 4 and 5.

Taking into consideration the calculated measures describing the structure of the data set and results of non-parametric estimation, an attempt was made to fit to data the theoretical probability density function, with a shape similar to that in Figs. 4 and 5 and in conformity with the properties described by the basic measures of location, dispersion, asymmetry and concentration.

Parametric estimation, fitting of log-normal distribution

The theoretical form of the probability density function was selected to be the log-normal distribution, which is given by the following formula *(3)* [23]:

$$p(x) = \frac{1}{x\sigma\sqrt{2\pi}} e^{(-\ln x - \mu)^2 / 2\sigma^2} \quad (3)$$

The distribution parameters, i.e. the mean of logarithms of analysed variables (μ) and the standard deviation of logarithms of variables (σ), were estimated by the maximum likelihood method [23]. Figs. 6 and 7 present distributions for the temperatures of 600 and 650 °C, respectively, whereas the estimated mean and standard deviation levels are presented in Table 3.

The calculated log-normal distribution parameters became the basis for the estimation of parameters of the linear regression function, which was used to make a forecast for the time of 10^5 hours.

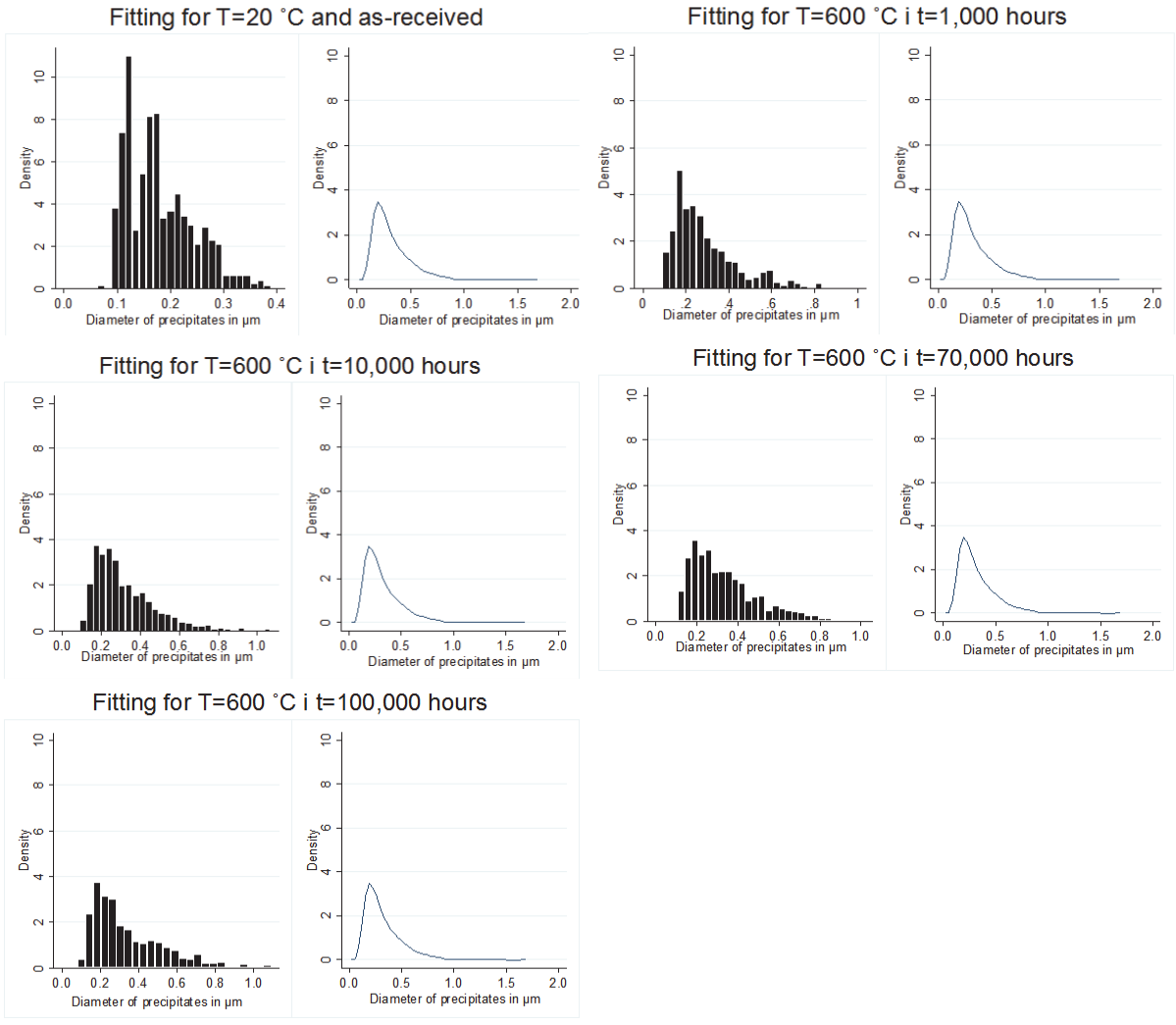

Fig. 4. Histograms and theoretical distributions for the temperature of 600 °C

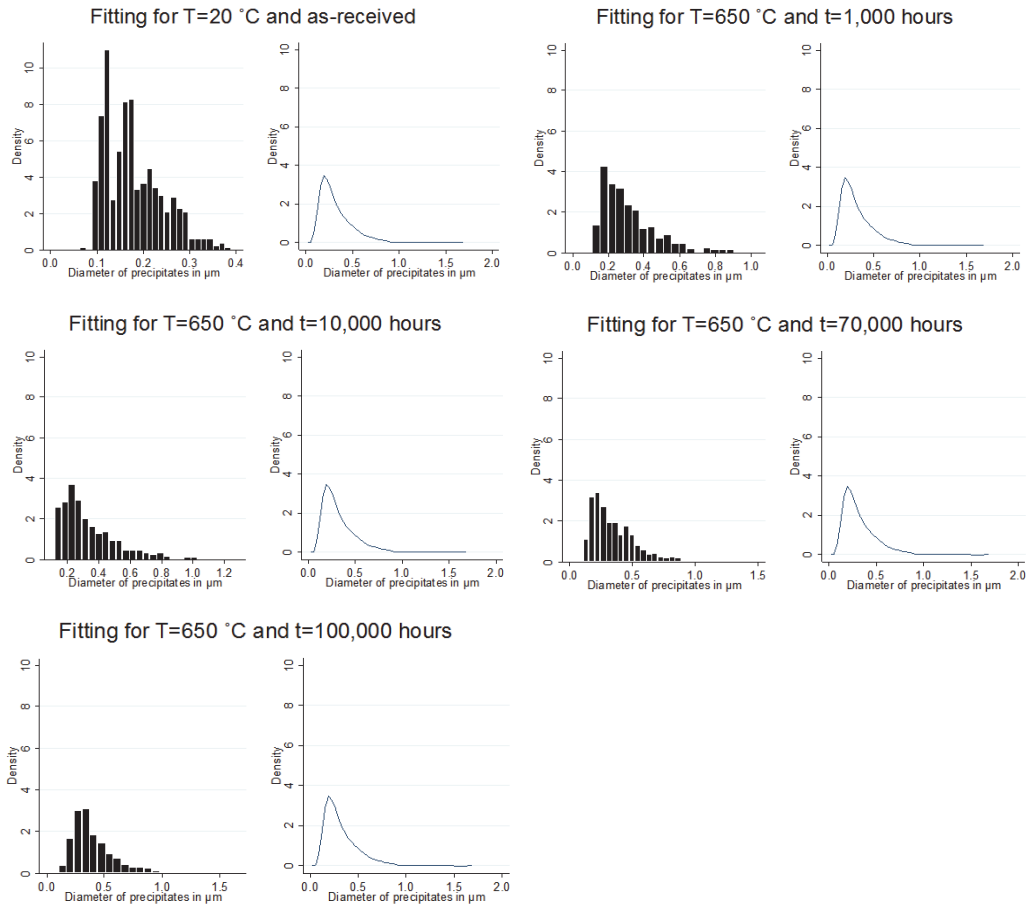

Fig. 5. Histograms and theoretical distributions for the temperature of 650 °C

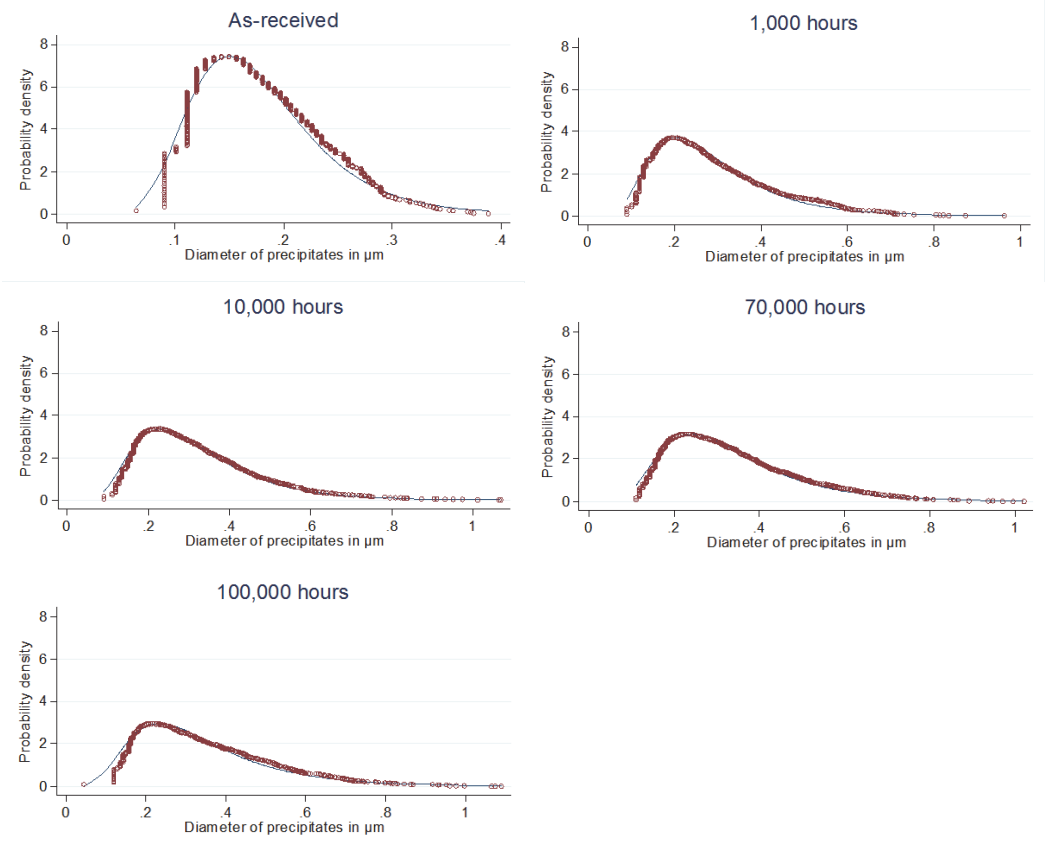

Fig. 6. Fitting of log-normal distribution for the temperature of 600 °C

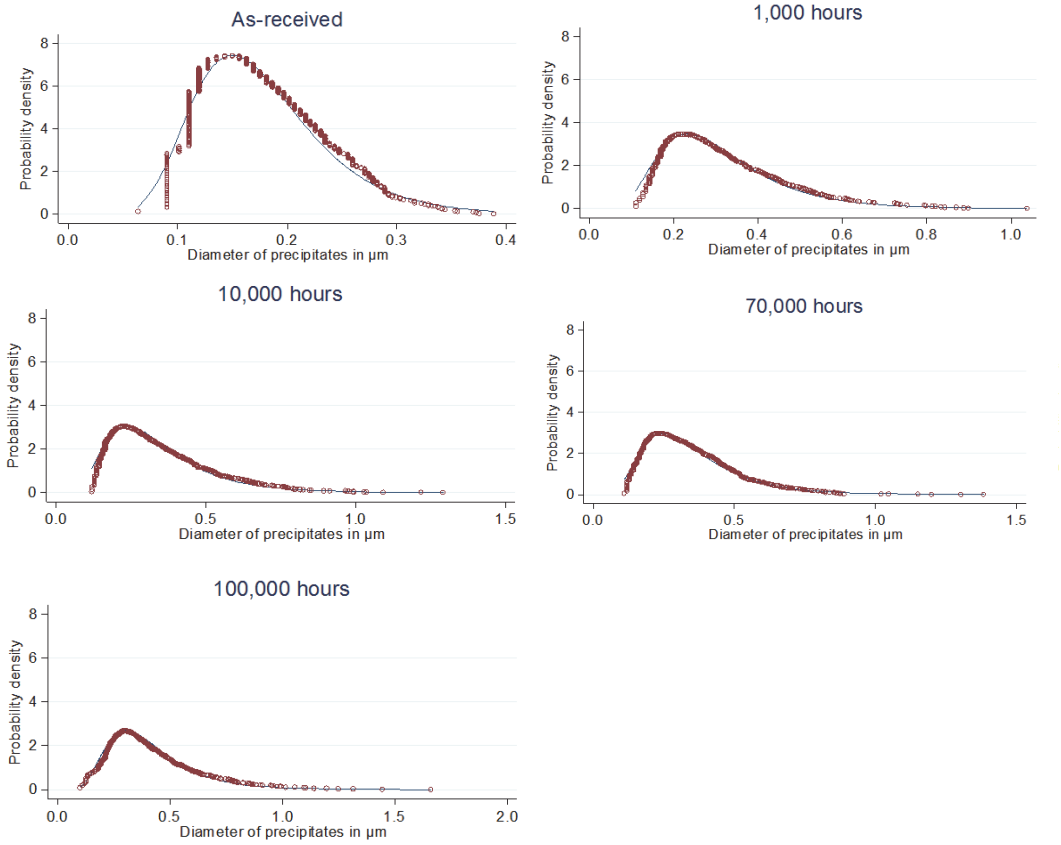

Fig. 7. Fitting of log-normal distribution for the temperature of 650 °C

TABLE 3

Calculated log-normal distribution parameters

	As-received	600 °C /1	600 °C /10	600 °C /70	600 °C /100	650 °C /1	650 °C /10	650 °C /70	650 °C /100
μ	-1.782	-1.3617	-1.2 485	-1.197	-1.194	-1.255	-1.195	-1.161	-0.987
σ	0.3371	0.4686	0.458	0.4648	0.506	0.444	0.486	0.479	0.439

3.3. Probability density forecast

The forecast of the expected value of precipitate diameter and its dispersion, including the average residual error and average *ex ante* prediction error, are shown in Fig. 8. The prediction error specifies the average fluctuations of the forecast variable, around the forecast made, which can be expected at the time it has been determined for. In the assumption, this error grows as the forecast horizon is being extended. Its high value indicates low stability of the analysed relationships.

The analysed relationship is linear on a logarithmic scale, but after delogarithmisation it takes the form of a power function. Thus, it is non-linear with regard to the variables and linear with regard to the regression function parameters. Also, the stability of parameters over time is assumed.

In Fig. 9, the fitting and forecast log-normal distributions are compared.

The analysis the results of which are shown in Fig. 9 reveals changes in the probability density function over time. The dynamics of these changes is significantly higher than that for the temperature of 650 °C.

4. Summary

The highest degradation in microstructure with reference to the as-received condition was observed after ageing at 650 °C for 10^5 h, which revealed a significant disappearance of martensite laths and increase in the amount and size of precipitates at the former austenite grain boundaries and at the remained or former martensite laths.

The quantitative analysis of selected characteristic images of microstructure allowed the database including precipitate diameters measured for two temperature levels: 600 and 650 °C, and at five moments, i.e. in the as-received condition and after ageing for 10^3, 10^4, $7*10^4$ and 10^5 h, to be developed. The collected results of investigations were the basis for carrying out the statistical structure analysis of the set. It

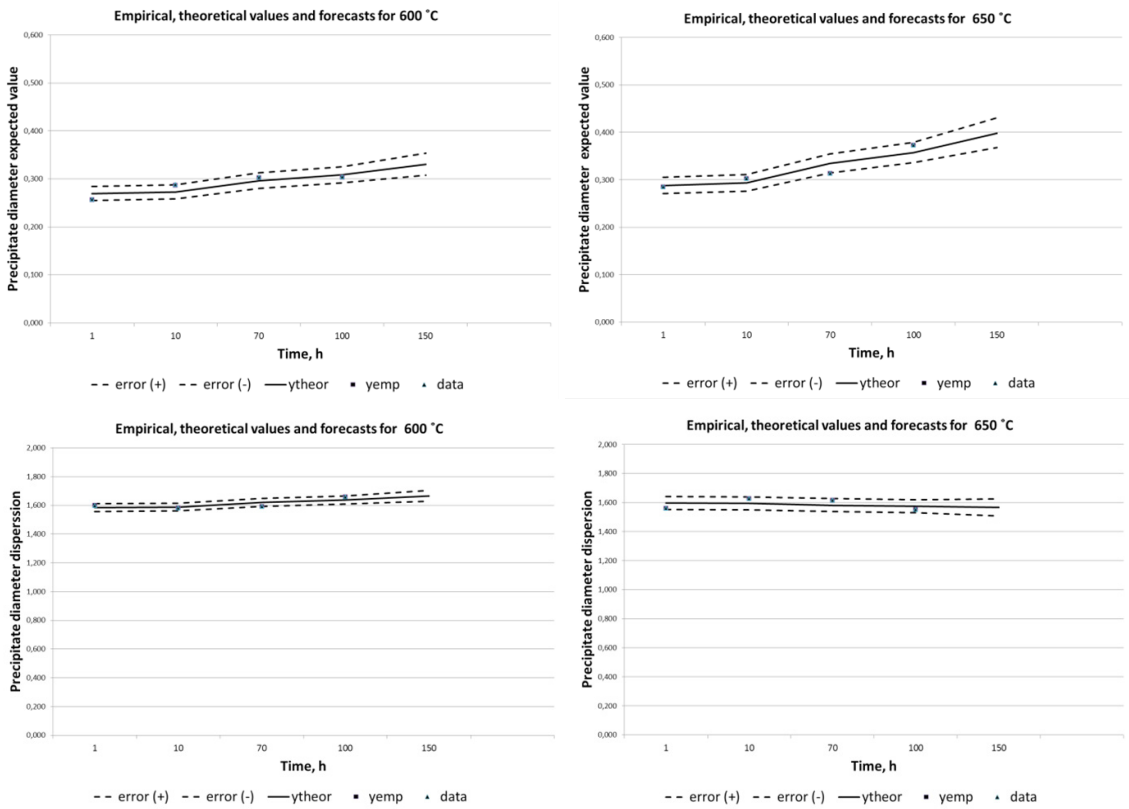

Fig. 8. Empirical and theoretical values and forecast for the mean and standard deviation of log-normal distribution of precipitate diameter

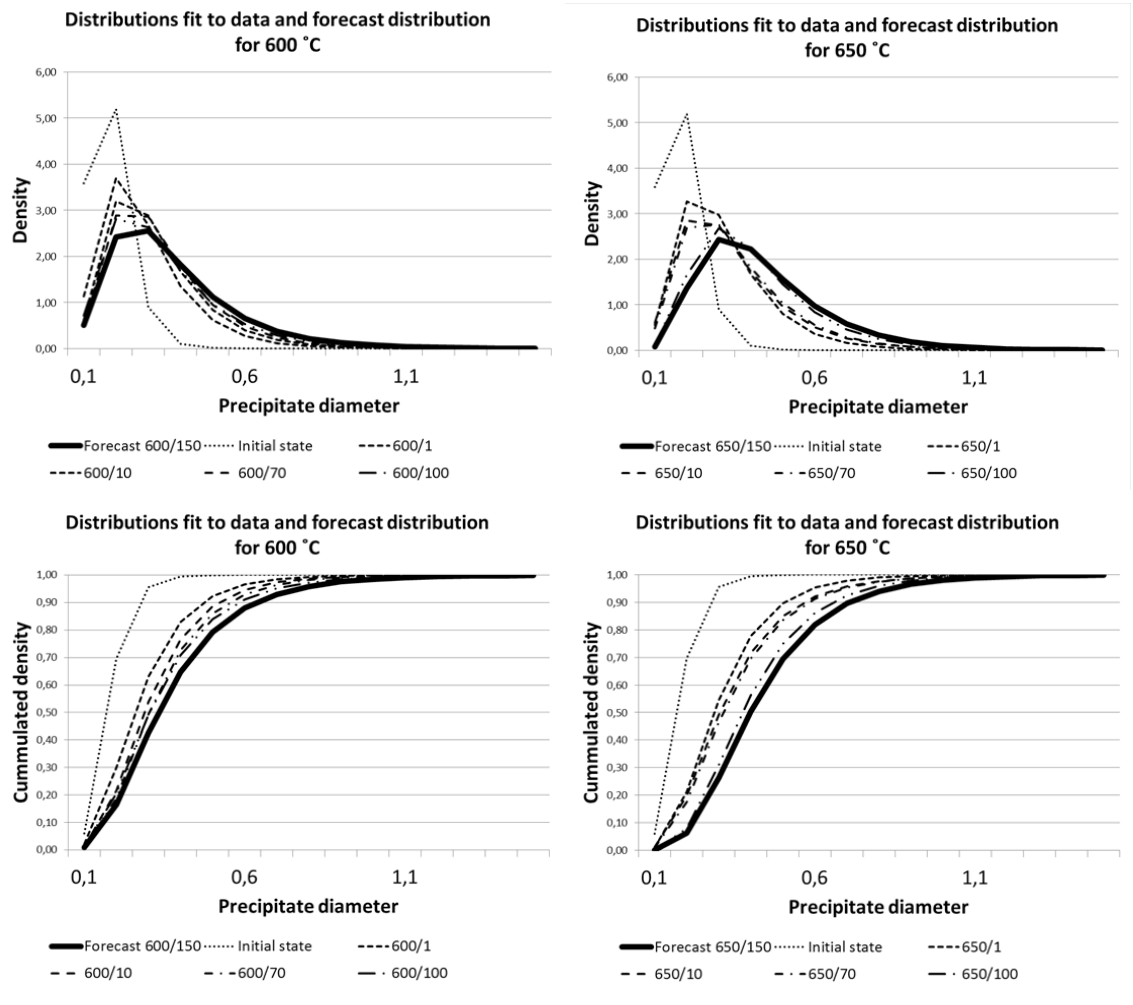

Fig. 9. Fit and forecast log-normal distributions of precipitate diameter

was demonstrated that the structure was changing in time, which was finally described by changes in the probability density function parameters. The formal description was made using the mathematical statistics methods, and the theory of forecasting was used.

The identification of changes in the microstructure required the classic assumptions adopted in the theory of prediction to be repealed. The basis for estimation of the parameters of the linear regression function, which was used to develop a forecast for the time of 10^5 h, was the mean and standard deviation of the precipitate diameter logarithms. These are parameters of the theoretical probability density function, in the form of a log-normal distribution, the levels of which were estimated based on real data.

The forecast about increase in the size of precipitates at a temperature similar to the that of the long-term service, i.e. 600 °C for $1.5*10^5$ h, indicates a continuous, but very slow growth of precipitates. Their average diameter changed after ageing for $1.5 *10^5$ h compared to the as-received condition by approx. 170nm (100%), whereas the increase in ageing temperature up to 650 °C indicated higher dynamics in the growth of precipitations. Their average diameter increased by approx. 240nm, which provides more than 150% increase compared to the as-received condition.

The evaluated density function parameters show very high similarity of the size of precipitates after ageing at 600 °C for 10^5 h to that after ageing at 650 °C for 10^4 h. Such a similarity provides the possibility of using the methods of forecasting by analogy in the evaluation of degradation degree for materials operated under creep conditions [16]. The results of performed analyses confirm the suitability of mathematical statistics and forecasting methods in this issue.

Acknowledgements

The results in this publication were obtained as a part of research co-financed by the National Science Centre under contract 2011/01/D/ST8/07219 – Project: „Creep test application to model lifetime of materials for modern power generation industry". This publication was co-financed by the Ministry of Science and Higher Education of Poland as the statutory financial grant of the Faculty of Mechanical Engineering SUT.

REFERENCE

[1] A. Hernas, J. Dobrzański, J. Pasternak, S. Fudali, Characteristics of the new-generation materials for the power industry, Publishing House of the Silesian University of Technology, Gliwice 2015.

[2] T. Tański, K. Labisz, B. Krupińska, M. Krupiński, M. Król, R. Maniara, W. Borek, J. Therm. Anal. Calorim. (2015) DOI 10.1007/s10973-015-4871-y, (in press).

[3] J. Dobrzański, Open Access Library, Materials science interpretation of the life of steels for power plants, Gliwice 2011.

[4] L. Blacha, K. Michałek, A. Smalcerz, M. Warzecha, Metalurgija **53,** (4), 574-576 (2014).

[5] L.A. Dobrzański, A. Grajcar, W. Borek, Mater. Sci. Forum. **638-642**, 3224-3229 (2010).

[6] A. Zieliński, G. Golański, M. Sroka, P. Skupień, Mater. High Temp. **33**, (2), 154-163 (2016), DOI: 10.1080/09603409.2016.1139306 (in press).

[7] M. Król, P. Snopiński, B. Tomiczek, T. Tański, W. Pakieła, W. Sitek, P. Est. Acad. Sci. **65**, (2), 107-116 (2016).

[8] M. Król, T. Tański, W. Sitek, Mater. Sci. Eng. **95,** (2015), DOI:10.1088/1757-899X/95/1/012006 (in press).

[9] Z. Brytan, J. Niagaj, Chiang. Mai. J. Sci. **40, (**5), 923-937 (2013).

[10] X. Guo, J. Gong, Y. Jiang, X. Wang, Y. Zhao, Mater. High Temp. (2015), DOI:1878641315Y-0000000003 (in press).

[11] P.F. Giroux, F. Dalle, M. Sauzay, J. Malaplate, B. Fournier, A.F. Gourgues-Lorenzon, Mat. Sci. Eng. A-Struct. **527,** (16), 3984-3993 (2010).

[12] L.A. Dobrzanski, R. Maniara, J. Sokolowski, W. Kasprzak, M. Krupiński, Z. Brytan, J. Mater. Process. Tech. **192,** 582-587 (2007).

[13] J. Hald, Int. J Pres. Ves. Pip. **85,** (1), 30-37 (2008).

[14] L.A. Dobrzański, W. Borek, Mater. Sci. Forum. **654-656**, (1-3), 266-269 (2010).

[15] H. Adrian, J. Augustyn-Pieniążek, P. Marynowski, P. Matusiewicz, Hutnik, Wiadomości Hutnicze **81**, (4), 208-214 (2014).

[16] A. Zieliński, G. Golański, M. Sroka, J. Dobrzański, Mater. Sci. Tech-Lond. (2015), DOI: 10.1179/1743284715Y.0000000137 (in press).

[17] A. Zieliński, M. Miczka, M. Sroka, Mater. Sci. Tech-Lond., 2016, DOI:10.1080/02670836.2016.1150242 (in press).

[18] W. Sitek, T. Famena. **34**, (3), 39-46 (2010).

[19] A. Zieliński, G. Golański, M. Sroka, Kovove Mater. **54**, (1), 61-70 (2016).

[20] A. Zieliński, M. Miczka, B. Boryczko, M. Sroka, Arch. Civ. Mech. Eng. 2016, DOI:10.1016/j.acme.2016.04.010 (in press).

[21] N.J. Cox, Stata. J. **5**, (2), 259-273 (2005).

[22] I.H. Salgado-Ugarte, M. Shimizu, T. Taniuchi, Stata. Tech. Bull. **3**, 155-173 (1993).

[23] M. Fisz, Probability theory and mathematical statistics, John Wiley and Sons, 1980.